

Impact of glacier changes on the local gravity field by numerical forward modelling and applicability studies using GOCE gravity gradients for regional gravity field solutions by Least Squares Collocation



Florian Heuberger and Daniel Rieser

Abstract

A numerical approach to gravity forward modelling is developed and introduced in order to investigate the effects of ice mass changes on the local gravity field. These studies are based on a synthetic glacier model of the northern island of Novaya Zemlya, which incorporates geometrical as well as 3D-density information. By modifying the model parameters like ice thickness and the density distribution in the interior of the ice body, the changes that can be expected in the gravity signal are estimated. Furthermore, different assumptions on the underlying bedrock topography can also be evaluated with respect to the resulting gravity signal. Simulations with realistic model parameters yield to gravity attraction differences in the order of a few mGal. Based on given digital elevation models featuring ice mass changes within the last 60 years, the forward modelling approach allows the investigation of the impact of ice change on the gravity field. The estimated effect on the gravity field reaches a maximum amplitude of 6 mGal over the whole period, implying an average change of 1 mGal per decade. In addition, a concept for using gradient observations of ESA's satellite mission GOCE for regional gravity field determination is introduced in this paper. In contrast to the official objectives, i.e. the generation of a global static gravity field based on the entirety of observations, here the measurements are introduced as in situ observations over a spatially restricted area and the gravity field is determined by means of Least Squares Collocation. For this purpose the noisy gradient data are filtered using the Wiener approach and the covariance functions required for collocation are derived. Furthermore, the problematic issue of the coordinate frame is discussed and a possible solution is presented. Finally, a gravity field solution based on real GOCE gradient data for November 2009 is generated for the above mentioned study area in terms of gravity anomalies. With this method and the chosen data configuration it is possible to determine the gravity field with an estimated accuracy of 4 mGal. The difficult comparison of gravity attractions from numerical forward modelling and gravity anomalies from the space-borne gradiometry is discussed.

Keywords: Numerical forward modelling, gravity field, ice mass change, least squares collocation, GOCE

Kurzfassung

Um die Auswirkungen von Eismassenvariationen auf das lokale Schwerfeld zu untersuchen, wird ein numerischer Ansatz zur Schwere-Vorwärtsmodellierung entwickelt und vorgestellt. Diese Untersuchungen bauen auf einem synthetisch generierten Gletschermodell für die Nordinsel der Novaya Zemlya Inselgruppe auf, das sowohl die geometrische Struktur als auch die 3D-Dichteverteilung beinhaltet. Durch Modifikationen der Modellparameter wie Eisdicke und Dichteverteilung im Eiskörper werden die zu erwartenden Veränderungen im Schweresignal untersucht. Die modellierte Topographie des Felsuntergrundes kann ebenfalls hinsichtlich unterschiedlicher Annahmen auf Differenzen im resultierenden Schweresignal betrachtet werden. Die Simulationen mit realistisch angenommenen Modellparametern ergeben Gravitationsunterschiede von wenigen mGal. Weiters wird mit Hilfe des Vorwärtsmodellierungsansatzes die Auswirkung der Eismassenveränderungen der letzten 60 Jahre untersucht, die in Form von zwei digitalen Geländemodellen gegeben sind. Der abgeschätzte Effekt auf das Schwerfeld erreicht eine maximale Amplitude von 6 mGal über den gesamten Zeitraum, bzw. eine durchschnittliche Veränderung von ca. 1 mGal pro Jahrzehnt. In weiterer Folge wird in diesem Beitrag ein Konzept vorgestellt, wie Gradientenbeobachtungen der ESA Satellitenmission GOCE für eine regionale Schwerfeldlösung verwendet werden können. Im Gegensatz zur offiziellen Zielsetzung, der Bestimmung eines globalen statischen Schwerfelds basierend auf der Gesamtheit aller Beobachtungen, werden hier die Messungen als Direktbeobachtungen über einem räumlich begrenzten Gebiet eingeführt und die Schwerfeldlösung über die Methode der Kollokation nach kleinsten Quadraten errechnet. Dazu werden die rauschbehafteten Gradientendaten nach dem Wiener-Ansatz gefiltert und die für die Kollokation notwendigen Kovarianzfunktionen abgeleitet. Weiters wird die Problematik des Koordinatenrahmens diskutiert und ein möglicher Lösungsansatz vorgestellt. Mit einem realen GOCE Gradienten Datensatz für November 2009 wird eine Schwerfeldlösung in Form von Schwereanomalien für das oben genannte Untersuchungsgebiet berechnet. Mit der verwendeten Meth-

ode und Datenkonfiguration kann das Schwerefeld mit einer geschätzten Genauigkeit von 4 mGal bestimmt werden. Die schwierige Gegenüberstellung der beiden Ansätze (Gravitation aus Vorwärtsmodellierung und Schwereanomalien aus Satellitengradiometrie) wird diskutiert.

Schlüsselwörter: Numerische Vorwärtsmodellierung, Schwerefeld, Eismassenveränderung, Kollokation nach kleinsten Quadraten, GOCE

1. Introduction

The knowledge of the (regional) gravity field is an important factor for the observation and interpretation of ice mass changes in the context of climate change. The ice mass balance is commonly derived from geometrical information of the ice bodies, which is observed and mapped by different methods [1]. Amongst those are space-borne altimetric missions like ICESat, CryoSat-2 as well as interferometric concepts like ERS-ENVISAT, TanDEM-X or TerraSAR-X. For such remote sensing and mapping methods a precise static gravity field expressed in terms of geoid heights provides a common solid height datum which is aimed to be known with highest accuracy.

Additionally, mass changes like those of the snow and ice resources also have a direct impact on the gravity field, since gravity is related to mass distribution within the Earth and at its surface. With the launch of the satellite mission Gravity Recovery and Climate Experiment (GRACE) [2] in 2002, the gravity field can also be observed with respect to its temporal variations. These can inversely be related to the mass transports from geodynamic processes [3, 4]. However, the separation of the gravity effect caused by a distinct source of mass change like ice cover variations from the overall gravity signal still poses a scientific problem, which is amplified by the so called leakage effect, explained e.g. in [5, 6].

In this context two aspects of the gravity field are investigated and presented in this paper: on the one hand (section 2), local changes in the gravity field caused by variations of ice masses can be modelled by numerical forward modelling. Based on a realistic simulation of an ice body's structure, the gravity field effects are estimated. Also, temporally changing mass distributions, e.g. variations in the snow-ice cover, are treated. Thus, also the gravity field accuracy required to sense such (temporally varying) signals can be estimated.

On the other hand, the ESA satellite mission Gravity field and steady state Ocean Circulation Explorer (GOCE) [7] offers new opportunities for accurate static gravity field solutions. The objective of GOCE is the determination of a global

gravity field. However, such a global approach might smooth local or regional features of the gravity field to some extent. Furthermore, satellite gravity missions can only deliver gravity information limited in spectral and spatial resolution (about 80 km are expected from GOCE). Therefore, a combination of terrestrial, air-borne and satellite gravity data is commonly performed [8] for regional gravity field determinations to overcome these limitations. The method of Least Squares Collocation (LSC) offers such an opportunity for data combination. In section 3, an approach for the inclusion of the novel gravity gradient data type of the GOCE mission in a LSC process is introduced and a regional gravity field on solely gradient data is computed.

For the research presented in this paper, Novaya Zemlya has been selected as principal study region (Fig. 1). The northern part of the island is covered by the world's third largest ice body of about 22 000 km² (cf. [9]). The main causes for selecting this region were the availability of detailed digital elevation models for the forward modelling as well as the dense GOCE ground tracks (high spatial density of gravity gradient observations) at this high geographical latitude.

Section 4 of this paper includes a discussion of the intermediate results of both approaches and their comparison. Section 5 contains the conclusions, and an outlook is given on possible applications and further studies.



Fig. 1: The study region Novaya Zemlya (Source: Marble).

2. Numerical Forward Modelling

2.1 Mathematical Background

A closed formula for a rectangular prism's gravity effect on an arbitrarily defined computation point can be derived from Newton's integral formula describing the attraction exerted by a solid body, as described in [10]. The formula for the gravity anomaly Δg depending on the relative density $\Delta\rho$ is based on using all eight prism corners ($x_{1,2}$, $y_{1,2}$, $z_{1,2}$ in a local horizontal system with its origin at the computation point) for the integral solution, as described in [11]

$$\Delta g = -G\Delta\rho \left[x \ln(y+r) + y \ln(x+r) - \right. \quad (1)$$

$$\left. - z \arctan \frac{xy}{zr} \right] \Bigg|_{x_1}^{x_2} \Bigg|_{y_1}^{y_2} \Bigg|_{z_1}^{z_2}$$

where G denotes the Newton gravitational constant and r is the distance between the computation point and the currently evaluated corner of the prism.

By summing up the resulting gravity anomalies Δg of all individual prism elements of a digital terrain model (DTM) for one particular computation point, the sum yields the model's gravity effect on this point. This process is of course well known in remove-restore techniques for gravity field computation (cf. [12]). However, usually a constant density value 2.67 g/cm^3 is applied. In this paper, we use a three-dimensional density distribution, i.e. prisms of different density (Fig. 2) leading to an absolute synthetic gravity field effect instead of terrain reduction. This modelling strategy will allow computing the contributions of bedrock and (changing) ice separately. Due to combination of DTM and 3D-density, we speak of a digital terrain density model (DTDM).

By defining a whole grid of computation points situated on the prism tops or on a constant level above, a synthetic gravity field can be calculated representing the gravitational effect (gravity attraction) of the underlying DTDM

The model itself is defined in a WGS-84 based geographic grid with homogeneous spacing in both directions. In order to meet the requirements of the Cartesian coordinate based Eq. (1), a transformation of relevant model parts (mass selection radius 167 km) to a local level frame (North, East, Up) originating at the actual computation point is carried out. This ensures that all the masses are placed correctly during each calculation loop, with regard to the Earth's curvature

and the meridian convergence as "seen" from individual computation points.

2.2 Model Composition

As described above, numerical forward modelling relies on the surface geometry and a three-dimensional density distribution. The geometrical representation of Novaya Zemlya is a combination of different data sources: synthetic aperture radar, altimetry and various maps were compiled by Joanneum Research (cf. [13]), yielding a digital terrain model of the island. Additionally, the International Bathymetric Chart of the Atlantic Ocean (IBCAO) [14] was used for modelling the surrounding underwater topography. By merging both data sets, a detailed geometric model of Novaya Zemlya and its surroundings could be generated. Forward modelling can only reflect a relative part of the gravity signal (cf. discussions in section 4). While this would not pose a problem in classical remove-restore techniques, more masses had to be included in the computations in order to obtain realistic mGal-ranges for the comparison with (absolute) gravity data from the LSC-solution. Accordingly, the digital terrain and density model (DTDM) was expanded and incorporates masses down to a depth of 600 meters.

In order to combine geometry and density information, a 3D-separation into ice, bedrock and ocean, which are treated individually during the model compilation process, is performed. One example of a final DTDM is shown in Fig. 2. The 3D-separation procedure has several interfaces that can be used to customize the parameters of bedrock and ice regarding both geometry and density in order to simulate different model states. These different models allow the analysis of every individual parameter change in terms of gravity field changes. Due to the primary focus

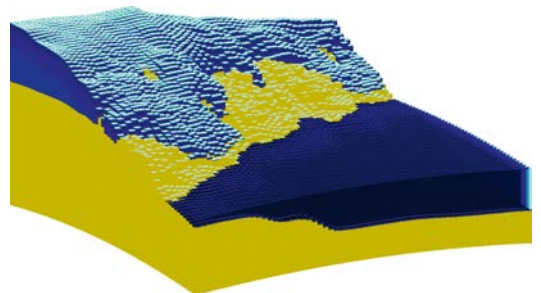


Fig. 2: Schematic close-up view of the digital terrain density model as "seen" from a computation point during numerical forward modelling, representing different densities for ice (cyan), bedrock (brown) and ocean (dark blue).

on ice mass change, the densities of bedrock and ocean were set to common constant values, whereas the ice density distribution relies on an empirical depth-density relation described more extensively in section 2.3 and [15].

2.3 Investigation of model parameters

The spatial resolution of the models used in this section is 0.5 km. A computation point for the gravity field forward modelling is situated directly on top of every (stacked) prism in the DTDM. All results in this section are gravity attractions g expressed in mGal. In the following paragraphs differences with respect to an “absolute” solution at epoch 2008 with default parameters are shown in the course of tuning the model parameters.

2.3.1 Changes in Ice Geometry

First, we simulated an ice loss of 10 % at the main ice cap which would result in a gravity field change in the range of 3 mGal (Fig. 3). This relative ice loss corresponds to about 40 to 50 m at the thickest parts of the ice sheet. Note that the ice thickness and therefore the underlying bedrock topography in this modelling process are based on the generic lookup table (LUT) described below. The positive changes in the gravity attractions are due to the fact that the computation points – in these forward modelling differences – are located directly on the surface of the DTDMs to asses the observable signal change, e.g. with terrestrial measurements that might be executed in situ. The computed ice mass loss results in lower altitudes on the second model and therefore in increased gravity attractions.

2.3.2 Bedrock Height

A LUT is used to model the bedrock height below the ice cap depending on the surface height given in the DTM. Two different LUT settings were compared in Fig. 4 to analyze the impact

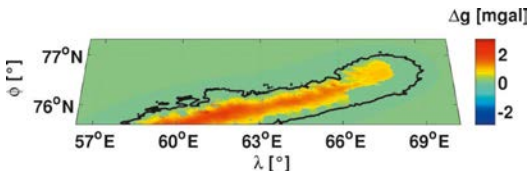


Fig. 3: Gravity attraction differences (in mGal) to be expected from an assumed ice mass loss of 10 % over the whole study area simulated via numerical forward modelling. Positive values (differences) are due to the lower altitude of computation points, where the surface height is decreasing due to the ice loss.

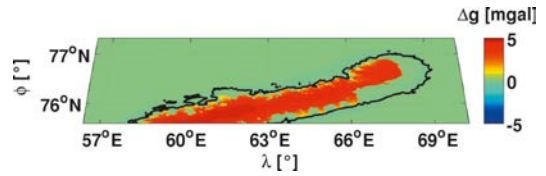


Fig. 4: Gravity attraction differences (in mGal) to be expected between different models for the bedrock topography below the ice caps simulated via numerical forward modelling (computed on the model surface).

of the LUT-parameters on the gravity field computation. In both cases a second order polynomial was used to compute the height of bedrock below a given surface height. These assumptions are based on observations performed by Joanneum Research ([17]). The impact on the computed gravity field amplitude is caused by the different bedrock height settings (differences of about 50 m at the areas with maximum DTM elevation) via the LUTs.

2.3.3 Ice Density Model

In order to achieve a realistic density distribution within the ice body, the empirical relation for a density ρ at a depth z , published by [16] is used

$$\rho(z) = \rho_i - (\rho_i - \rho_s) \exp\left(-\frac{1.9}{z_i} z\right). \quad (2)$$

The different parameters were defined in accordance with in situ measurements carried out by Joanneum Research in 2008 in the study region: the mean density of ice ρ_i (empirically determined), the surface snow density ρ_s , and the site dependent firn-ice transition depth z_i . The underlying measurements are described in [17]. Quantization into six bins allowed the top down density modelling by means of stacked prisms.

Due to its low firn-ice transition depth, the model has only a thin hull of lighter snow and ice above a solid ice core with constant density. The negligible impact of less than 1 mGal caused by different firn ice transition depths for the Schytt model is analyzed in [15].

2.4 Ice Change during the past 60 years

A combination of maps dated around 1950 and present remote sensing data allowed Joanneum Research [18] the mapping of spatially distributed ice change during the past 60 years (Fig. 5). Of course this map cannot be regarded as completely error free due to the large time span covered (with few historical datasets available) and might overestimate certain surface changes.

The implementation of this geometry variation within our numerical forward modelling frame-

work allows the computation of this surface elevation change interpreted as ice mass gain/loss in terms of gravity attractions (Fig. 6). The maximum signal amplitude change of about 6 mGal can be observed at the northern ice cap. This corresponds to about 1 mGal signal variation per decade. Regarding the spatial extent of the northern ice cap's signal change, a region of roughly 800 km² is mainly affected by these significant amplitudes.

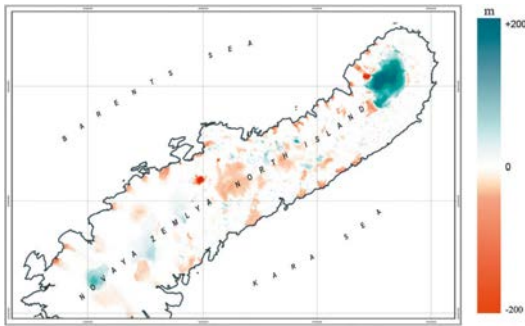


Fig. 5: Differences between elevation models of 1950s and 2008 in meters (Joanneum Research).

Note that the stations for these computations were held at an ellipsoidal height of 1500 m. This height was kept constant in order to avoid misinterpretations due to local gravitational effects acting on computation points directly at the surface of the different DTDMs. Additionally, the smaller absolute differences compared to Fig. 3 are also due to the smaller lateral extent of the observed surface changes opposed to a simulated melting over the whole study region.

3. Gravity field determination using GOCE gradients with Least Squares Collocation

The numerical forward modelling approach described in the previous sections allows a computation of gravitational effects based on a known or assumed topography and density distribution in the upper lithosphere. However, this reflects only a subset constituent of the actual gravity signal, which is a product of all masses inside the Earth and on its surface according to New-

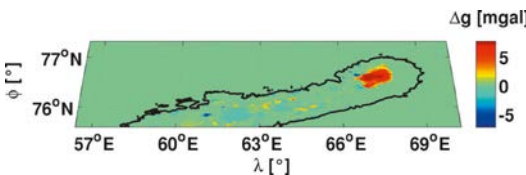


Fig. 6: Gravity attraction differences (in mGal) corresponding to the observed surface elevation changes since 1950 (computed using numerical forward modeling at a constant computation height of 1500 m).

ton's law of gravitation. The overall gravity signal can only be observed by terrestrial, air-borne or space-borne gravimetric measurements. As direct observations of the actual gravity are rare in remote regions, a space-borne technique like GOCE [7], launched in March 2009, offers a possibility to obtain information about the actual gravity field also in our study area. This mission is dedicated to determine the static global gravity field, which is accomplished by the European GOCE Gravity Consortium in the frame of the ESA project 'GOCE HPP' [19]. In this context the GOCE mission is expected to provide accurate gravity information, which is superior to other data types, especially in the medium wavelength spectrum of about degree and order 100 to 250 in terms of a spherical harmonic series expansion, which corresponds to 200 km to 80 km half wavelength of the gravity signal. The key instrument of the GOCE mission is the gradiometer. This assembly allows to measure gravity gradients, i.e. second order derivatives of the gravitational potential, from space. In contrast to the GOCE HPP solution strategies for deriving a global gravity field, the methods and concepts for the use of GOCE gradient data as in situ observations in the frame of local geoid computations are presented in this section.

3.1 Least Squares Collocation (LSC)

At regional scale, LSC [20] is a standard method for the computation of the Earth's gravity field. Its ability to combine various kinds of gravity field observations, e.g. geoid undulations, gravity anomalies or gravity gradients as measured by GOCE, is the major strength of this approach.

According to the theory of LSC, any arbitrary gravity field signal s can be predicted, if the linear functional which relates the signal to the basic disturbing potential T is applied to the covariance model of T in terms of a covariance propagation. The basic formula of LSC is given by

$$s = C_{sl}(C_{ll} + C_{nn})^{-1}l \tag{3}$$

where C_{sl} consists of the cross-covariances between the signal s and the observation l , while C_{ll} is the auto-covariance matrix of the signal content of the observations. The error structure of the observations is introduced by the noise-covariance matrix C_{nn} . The entries of C_{sl} and C_{ll} can be calculated from a covariance function of the anomalous potential

$$C(r_i, r_j, \psi_{ij}) = \sum_{n=N_{min}}^{N_{max}} k_n \left(\frac{R^2}{r_i r_j} \right)^{n+1} P_n(\cos \psi_{ij}). \tag{4}$$

It depends on the radius R of a sphere completely enclosed by the Earth, the distances r_i , r_j from the geocenter to the observation stations, and the Legendre polynomials P_n of degree n , which are functions of the cosine of the spherical distance ψ_{ij} between the stations. The signal variances k_n can for instance be obtained from the fully normalized harmonic coefficients of an a-priori gravity field model via the relation

$$k_n = \sum_{m=0}^n \left(\bar{C}_{nm}^2 + \bar{S}_{nm}^2 \right). \quad (5)$$

While the functional that relates the vertical gravity gradient T_{ZZ} to the anomalous potential T is simply given by the second order radial derivative, the functionals for all other gradients are more complex. For instance, the T_{XX} gradient can be expressed in terms of spherical coordinates by

$$T_{XX} = \left(\frac{1}{r} \frac{\partial}{\partial r} + \frac{1}{r^2} \frac{\partial^2}{\partial \varphi^2} \right) T. \quad (6)$$

To derive the covariance between gradients T_{XX} at different positions, the functional of Eq. 6 has to be applied twice to the covariance function in Eq. 4, once for each position, leading to

$$\text{cov}(T_{XX}, T_{X'X'}) = \left(\frac{1}{r} \frac{\partial}{\partial r} + \frac{1}{r^2} \frac{\partial^2}{\partial \varphi^2} \right) \left(\frac{1}{r'} \frac{\partial C}{\partial r'} + \frac{1}{r'^2} \frac{\partial^2 C}{\partial \varphi'^2} \right). \quad (7)$$

It can be seen, that the covariance propagation for gravity gradients requires partial derivatives of the basic covariance model C up to a maximum order of four. To calculate all necessary covariances of derivatives of T , an approach as in [21] can provide a convenient solution of the problem. An advantage of this approach is the possibility to perform covariance propagation to another reference frame quite easily. This fact is of great importance and will be applied in the next section.

3.2 Methodological restrictions and their solutions

Before GOCE gradient data can be used in LSC, it has to be considered that the six accelerometers of the gradiometers only show good performance in the measurement bandwidth between 5 and 100 mHz. The gradient data comprise measurement errors in terms of coloured noise in particular in the long-wavelength fraction of the gravity signal. To reduce these effects a filtering step has to be introduced. Here the standard Wiener filter method for filtering GOCE gravity gradients, explained in detail in [22] and [23], is adapted for the data set within the investigated region. It should be mentioned that this

approach requires a signal that is stationary in time, which has to be considered next.

A further major issue when dealing with GOCE data is the fact that the GOCE mission observes gravity gradients in the sensor frame called Gradiometer Reference Frame (GRF), where stationarity is not given in strict sense. However, this requirement would be fulfilled in the Local Orbit Reference Frame (LORF), which is defined by the actual flight direction of the satellite. GRF is deviating from LORF by several degrees (cf. [24]), so a preceding frame transformation would be necessary before filtering the gradient data.

Furthermore, gravity field quantities are derived with LSC in a Local North Oriented Frame (LNOF), defining a local geographical coordinate frame. In the case of the GOCE gradiometer, unfortunately not all of the gravity gradient components can be measured with the same level of accuracy. In fact, the accuracy of the off-diagonal elements T_{XY} and T_{YZ} is degraded by a factor of 100 to 1000 [25]. Hence, a rotation of the gradient tensor from GRF to LORF or GRF to LNOF must be avoided. Otherwise the large errors of the off-diagonal elements would be propagated to all other components and drastically deteriorate the well-measured gradients [26]. Alternatively, the base functions (i.e. the covariance matrices) of LSC given in LNOF have to be rotated to the GRF or LORF, which can be performed as outlined in section 3.1.

As a consequence of the problems discussed above, different solution strategies can be considered [27]. For this study, the GRF is defined as the computational reference frame, while the theoretical requirement of a stationary gradient time series is neglected, cf. Fig. 7. This means, that the covariance matrix entries of C_{ll} and C_{sl} of the LSC procedure (cf. Eq. 3) related to gradient observations have to be rotated to GRF, while the Wiener filter is directly applied to the observed gradient time series. If one further assumes that the gradient components are uncorrelated amongst each other, the noise-covariance matrix C_{nm} can be set up by using the corresponding error covariance function, which can be derived via the filter error of the Wiener filter process [28].

3.3 Gravity field computation

In this study the GOCE Level-1b data set for November 2009 is used. GOCE is expected to improve the gravity field especially in the medium-wavelength. Therefore, in accordance to the remove-restore concept [12], long wave-length gravity signals are computed from the EGM2008

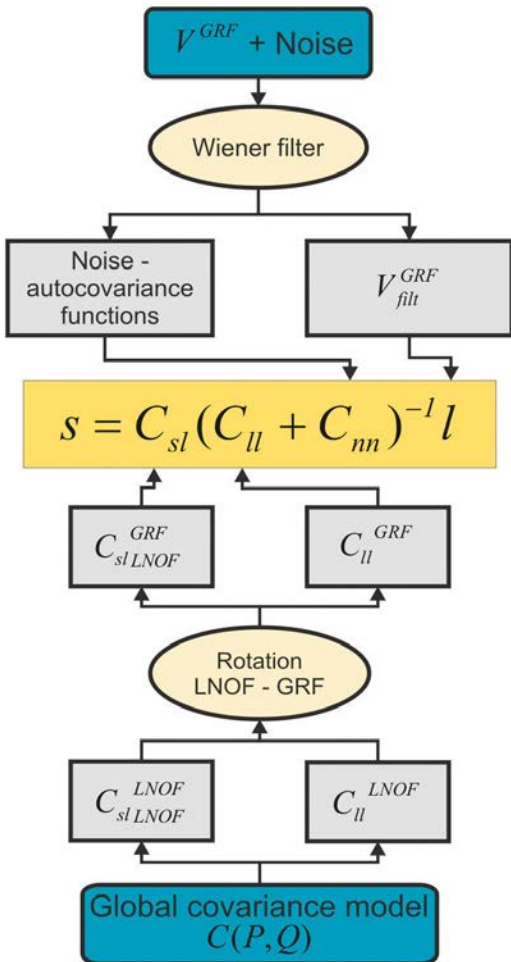


Fig. 7: Solution strategy for LSC applied in this study.

[29] gravity model up to degree and order (D/O) 49 in terms of spherical harmonics representation, and subtracted from the GOCE data beforehand. Thus it is implicitly assumed that the very long-wavelength component can be reduced by external gravity field information, e.g. derived by GRACE (which is integrated in EGM2008) very precisely in the low degrees. This assumption has been made since for this regional collocation study, the gravity data given in an area of such limited extent do not adequately represent the very long wavelength signal. Although GOCE will be superior to other data types only at higher degree and orders from around D/O 100 to maximum 250 (which corresponds to a spatial resolution of 80 km), in this case spectral information starting at D/O 50 is used. Hence, using GOCE data at these low degrees may not be an optimal

choice, but guarantees that most of the detectable gravity signal is used in this investigation.

The gravity field solutions are generated from GOCE gradient data of the main diagonal tensor components T_{xx} , T_{yy} and T_{zz} . Following the solution strategy introduced in the preceding section, each gradient time series is first filtered in the GRF by applying the Wiener filter method. The resulting Power Spectral Densities (PSDs) reflecting the signal content per frequency are exemplarily depicted for the T_{zz} gradient in Fig. 8. The noise-free reference gradient signals (blue), which are required for Wiener filtering, are simulated from EGM2008, D/O 50 to 250, while the noise PSDs (green) are an adaptation of the ones used in [25]. The resulting spectral content of the filtered signal (magenta curve) is very close to the one of the noise free reference in the measurement bandwidth.

To reduce computational efforts, the gradient data is thinned out from a sampling rate of originally 1 second to 5 seconds, and the test area is restricted to 53°–69°E and 73°–78°N, covering the Northern island of Novaya Zemlya, which is displayed in Fig. 9, bottom.

For the derivation of the covariance matrices C_{sl} and C_{ll} degree variances of EGM2008 consistent to the spectral information content of the observations from D/O 50 to 250 are used. The noise covariance matrix C_{mm} is set up in GRF using the error covariance functions of the Wiener filtering.

The gravity field solution based on this input data configuration is shown in Fig. 9, top, in terms of gravity anomalies. Note that the preliminary removed long-wavelength gravity constituent is not restored in this plot, thus the result depicts the impact of GOCE gradient data within the measurement bandwidth of the gradiometer instrument only. The result shows a strong gravity signal over the island with maximum val-

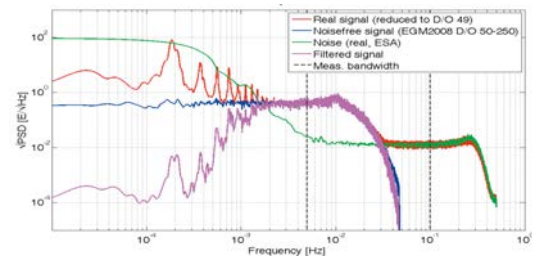


Fig. 8: PSD of GOCE T_{zz} gradients in GRF from D/O 50 to 250: real GOCE data (red), simulated from EGM2008 (blue), noise from ESA (green) and filtered (magenta).

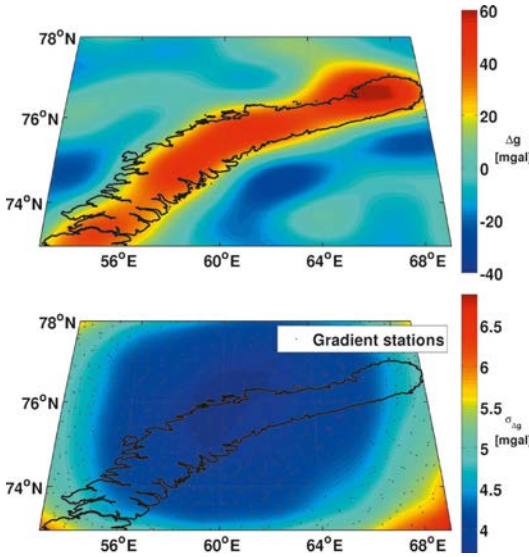


Fig. 9: top, Gravity field solution in terms of gravity anomalies (in mGal) from GOCE main diagonal gradient tensor components (November 2009) representing the spectral content from D/O 50 to 250; bottom, Corresponding standard deviation in mGal and data distribution of observations over the test area.

ues on the northern ice cap. The standard deviations (Fig. 9, bottom) are in the order of about 4 mGal, in the central region of the study area. The decreasing accuracy towards the borders of the test region can be explained with windowing effects of the LSC computation and is therefore not distressing.

4. Discussion of the results

In section 2, different model parameters of the forward modelling approach were investigated separately. Different assumptions for the bedrock structures beneath the ice body only have a negligible effect on the resulting gravity field (especially when looking at relative changes between two epochs). Even different parameter settings for the ice density model do not influence the computations (not shown in this paper), due to the shallow firn-ice transition depth in the study region. As the investigations with numerical forward modelling in section 2.3 have shown, a total ice mass loss in Novaya Zemlya of about 10 % would induce a gravity change in the order less than 3 mGal. The true ice change at the northern ice cap within the last 60 years (cf. section 2.4) has a gravity response of about 1 mGal/decade. This is by no means detectable by today’s gravity satellite missions for such small areas. For GRACE the temporally varying signals can

be resolved up to spectral degree and order 40 or 50, while higher frequency signals cannot be recovered due to the degrading signal-to-noise ratio of the mission with increasing degree [3]. Thus, only large mass variations can be detected by GRACE in e.g. Greenland, Alaska or Antarctica (cf. [27] and [28]) with a spatial resolution of several hundred kilometres.

The static regional gravity field solution with LSC is based on solely gravity gradient data from GOCE. The resulting achievable accuracy of 4 mGal (Fig. 9, bottom) is in correspondence with the accuracy of current official global GOCE HPF gravity field solutions [29]. Taking into account that the computation is only based on a very limited number of observations, this result can be regarded as very promising. However, despite GOCE is continuously (in contrast to the initial mission plans) observing gravity gradients with high precision in the spectral range between degree and order 50 and 250, this will not aid to improve the recovery of time variable signals. It has been shown in [30] and [31] that time variable signals from sources like ice mass variations are below the gradiometer error level. Recent studies conclude that only GOCE satellite-to-satellite tracking data will help to stabilize temporal GRACE solutions to some extent [32].

Finally, a coarse comparison between the gravity signal of the study area Novaya Zemlya resulting from the forward modelling approach (Fig. 10) and the computed gravity anomalies from LSC using GOCE gradients (Fig. 9, top) is performed. Beforehand, the results of numerical forward modelling had to be spatially filtered in order to allow a comparison despite the different spatial resolutions – while the high spatial resolution of the used DTDM (0.5 km posting) surpasses even the currently highest-degree model EGM2008 (maximum degree 2190, corresponding to 10 km), the LSC solution is limited to a spatial resolution of about 80 km. The filtered gravity field is slightly affected by the windowing effects of the Gaussian filter that was applied

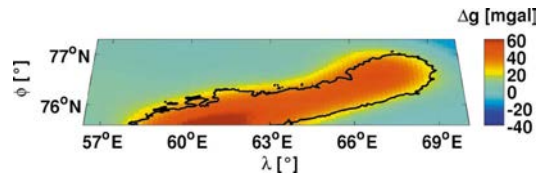


Fig. 10: Low-pass filtered gravity solution (gravity attractions g in mGal) computed by numerical forward modelling of ice (density model according to Schytt) and topographic masses down to a level of -600 m (constant density of 2.67 g/cm³).

to adapt the resolutions of the two computed gravity fields. Nevertheless, the general structures – in form of two distinct bulges with maximum amplitude along the main elevations of the ice body – are clearly discernible in both figures.

However, interpretations have to be done with care as several aspects have to be considered. First, the local modelling of mass prisms is mainly based on relative density contrasts in the upper lithosphere. Also, the modelled area is just a finite part of the whole Earth's mass and is therefore neglecting the influence of masses lying outside and underneath this region. In contrast, the LSC solution incorporates the integral gravity field, but only in the spectral range of degree and order 50 to 250. Thus, this is only a plausibility consideration of the results of both methods.

5. Conclusions and Outlook

For the estimation of the gravitational effects that can be caused by changing ice masses, a numerical forward modelling approach has been implemented and tested for the island of Novaya Zemlya. The investigated glacier model incorporates the 3D-geometry and assumed density distribution of the ice body and its surrounding topography. Simulations of mass change within the modelling process enable a better understanding of the impacts of ice mass variations on the gravity field. The amplitudes of these effects on the gravity field are – as expected – very small, especially with respect to their small spatial extent. Therefore, ice mass changes of the magnitude currently observed on Novaya Zemlya will be hard to detect by multi-temporal (mainly space-borne) gravity field solutions working on lower spatial resolutions. Nevertheless, numerical forward modelling can still be a valuable tool to aid the separation of ice-related gravity signals from the integral gravity variations as observed by GRACE, where it can help in isolating leakage effects.

In the second part of this paper the novel gravity gradient data type of the GOCE mission is integrated in the LSC process for regional gravity field determination independent of the reference frame. It is shown that a Wiener filter can reduce the coloured noise from gradient data on the one hand, and on the other hand delivers an adequate stochastic model of the measurement errors in terms of covariance functions. A regional gravity field solution with LSC based on solely real GOCE gradient data achieves an accuracy level similar to that of the current offi-

cial global gravity field solutions of GOCE HPF. Currently ESA is carrying out investigations to further refine the quality of the gravity gradient data. Hence, some potential improvements for the approach presented here might be expected. In future, GOCE gravity gradients shall be combined with other (terrestrial) data sources via LSC. First studies (not shown in this paper) have already stated the favourable impact of GOCE gradients on the accuracy of combined regional gravity field solutions.

Acknowledgments

The presented studies were part of the project Modelling Snow-Ice cover Evolution and Associated Gravitational Effects with GOCE constraints (ICEAGE) which was performed in the frame of the Austrian Space Application Programme (ASAP), Phase 5, funded by the Austrian Research Promotion Agency (FFG), project number 817106.

Without the help of our project partners and colleagues Aleksey Sharov (Joanneum Research), Prof. Roland Pail (now TU München), and Christoph Gisinger, these results would not have been achievable.

References

- [1] *Rignot E., Thomas R.H. (2002)*. Mass Balance of Polar Ice Sheets. *Science* 297, 1502, doi: 10.1126/science.1073888
- [2] *Tapley, B. D., Bettadpur S., Watkins M., Reigber C. (2004a)*. The Gravity Recovery and Climate Experiment: Mission Overview and Early Results. *Geophys. Res. Lett.*, Vol. 31, L09607
- [3] *Wahr J., Molenaar M., Bryan F. (1998)*. Time variability of the Earth's gravity field: Hydrological and oceanic effects and their possible detection using GRACE. *Journal of Geophysical Research*, Vol. 103, no. B12, pp 30,205-30,229
- [4] *Tapley, B. D., Bettadpur S., Ries J. C., Thompson P. F., Watkins M. M. (2004b)*. GRACE measurements of Mass Variability in the Earth System. *Science*, Vol. 305, no. 5683, 503-505
- [5] *Baur O., Kuhn M., Featherstone W. E. (2009)*. GRACE-derived ice-mass variations over Greenland by accounting for leakage effects. *Journal of Geophysical Research*, Vol. 114, B06407, doi:10.1029/2008JB006239
- [6] *Swenson S., Wahr J. (2003)*. Estimated accuracies of regional water storage variations inferred from the Gravity Recovery and Climate Experiment (GRACE). *Water Resources Research*, Vol. 39, No. 8, 1223, doi:10.1029/2002WR001808
- [7] *Drinkwater M., Foberghagen R., Haagmans R., Muzi D., Popescu A. (2003)*. GOCE: ESA's First Earth Explorer Core Mission. *Space Sciences Series of ISSI*, 18, p 419-432
- [8] *Pail R., Kührtreiber N., Wiesenhofer B., Hofmann-Wellenhof B., Of G., Steinbach O., Höggerl N., Imrek E., Ruess D., Ullrich C. (2008)*. The Austrian Geoid 2007. *VGI, Jahrgang 98, Heft 1/10*
- [9] *Sharov A.I. (2005)*. Studying changes of ice coasts in the European Arctic, *Geo-Marine Letters* 25, Springer,

- New York, 153–166, DOI 10.1007/s00367-004-0197-7
- [10] Hofmann-Wellenhof B., Moritz H. (2005). *Physical Geodesy*. Springer, Wien, New, York
- [11] Mader, K. (1951). Das Newtonsche Raumpotential prismatischer Körper und seine Ableitungen bis zur dritten Ordnung. Österreichische Zeitschrift für Vermessungswesen, Österreichischer Verein für Vermessungswesen. Sonderheft 11
- [12] Forsberg, R. (1984). A study of terrain reductions, density anomalies and geophysical inversion methods in gravity field modelling, Tech. Rep. 355, The Ohio State University, Columbus
- [13] Pail R., Sharov A., Rieser D., Heuberger F., Gisinger C. (2010). Modelling snow-ice cover evolution and associated gravitational effects with GOCE constraints (ICEAGE), Final Report. Technical report, FFG, Austrian Space Applications Programme
- [14] Jakobsson M., Macnab R., Mayer M., Anderson R., Edwards M., Hatzky J., Schenke H-W., Johnson P. (2008). An improved bathymetric portrayal of the Arctic Ocean: Implications for ocean modeling and geological, geophysical and oceanographic analyses, v. 35, L07602, Geophysical Research Letters, doi:10.1029/2008GL033520
- [15] Gisinger C., Heuberger F., Rieser D., Pail R., and Sharov A. (2010). Ice Mass Change versus Gravity – Local Models and GOCE's Contribution. In Living Planet Symposium Conference Proceedings, ESA
- [16] Schytt V. (1956). Summary of the glaciological work. In Report on glaciological investigations during the Norwegian-British-Swedish Antarctic Expedition, 1949-1952, Assn. Intern. Hydrologic, Vol. 4, IUGG, Rome, 236–243
- [17] Sharov A. I. (Ed., 2010). SMARAGD – Satellite Monitoring and Regional Analysis of Glacier Dynamics in the Barents-Kara Region, Joanneum Research, Printshop, Graz
- [18] Sharov A.I., Nikolskiy D. B. (2007). Semi-controlled interferometric mosaic of the largest European glacier, in Proceedings ENVISAT Symposium Montreux, 7, European Space Agency, SP-636
- [19] Rummel R., Gruber T., Koop R. (2004). High Level Processing Facility for GOCE: Products and Processing Strategy. In Proceedings 2nd International GOCE User Workshop, Frascati 2004, European Space Agency, Noordwijk, The Netherlands
- [20] Moritz H. (1980). *Advanced Physical Geodesy*. Wichmann Verlag, Karlsruhe
- [21] Tscherning C.C. (1993). Computation of covariances of derivatives of the anomalous gravity potential in a rotated reference frame. *Manuscripta Geodetica*, Vol. 18, no. 3, pp 115-123
- [22] Albertella A., Migliaccio F., Reguzzoni M., Sansò F. (2004). Wiener filters and collocation in satellite gradiometry. In International Association of Geodesy Symposia, '5th Hotine-Marussi Symposium on Mathematical Geodesy', (Ed. F. Sansò), vol. 127, Springer-Verlag, Berlin, 32-38
- [23] Papoulis A. (1984). *Signal analysis*. McGraw Hill, New York
- [24] Pail R. (2005). A parametric study on the impact of satellite attitude errors on GOCE gravity field recovery. *Journal of Geodesy*, 79, 231-241
- [25] Catastini G., Cesare S., De Sanctis S., Dumontel M., Parisch M., Sechi G. (2006). Predictions of the GOCE in-flight performance with the end-to-end system simulator. In Proc. 3rd International GOCE User Workshop, November 2006 Frascati, Italy, ESA SP-627, pp9-16
- [26] Müller J. (2003). GOCE gradients in various reference frames and their accuracies. *Advances in Geosciences*, 1, 33–38, doi:10.5194/adgeo-1-33-2003
- [27] Rieser D., Pail R. (2009). Using GOCE Gravity Gradients For A Combined Regional Gravity Field Solution With Least Squares Collocation, Poster presented at the IAG 2010, Buenos Aires
- [27] Velicogna, I., Wahr J. (2005). Greenland mass balance from GRACE. *Geophys. Res. Lett.*, 32, L18505, doi:10.1029/2005GL023955
- [28] Migliaccio F., Reguzzoni M., Sansò F. (2004). Space-wise approach to satellite gravity field determination in the presence of coloured noise. *Journal of Geodesy*, 78, 304-313
- [28] Velicogna, I., Wahr J. (2006). Measurements of time-variable gravity show mass loss in Antarctica. *Science*, 311, 1754–1756, doi:10.1126/science.1123785
- [29] Gruber T. (2011). GOCE Gravity Field and Orbit Results: The HPF Experience. Presentation at: 4th International GOCE User Workshop, 31 March – 1 April 2011, Munich, Germany
- [29] Pavlis N. K., Holmes S., Kenyon S., Factor J. (2008). An Earth Gravitational Model to Degree 2160: EGM2008, Poster presented at the 2008 General Assembly of the European Geosciences Union, Vienna
- [30] Abrikosov O., Jarecki F., Müller J., Petrovic S., Schwintzer P. (2006). The impact of temporal gravity variations on GOCE gravity field recovery. In: Flury J., Rummel R., Reigber C., Rothacher M., Boedecker G, Schreiber U (eds.), *Observation of the Earth system from space*. Springer, Heidelberg, pp 255–269
- [31] Bouman J., Rispens S., Gruber T., Koop R., Schrama E., Visser P., Tscherning C. C., Veicherts M. (2009). Preprocessing of gravity gradients at the GOCE high-level processing facility; *Journal of Geodesy*, Vol. 83, Nr. 7, pp 659-678, Springer, ISSN 0949-7714, DOI: 10.1007/s00190-008-0279-9
- [32] Pail R., Fecher T., Jäggi A., Goiginger H. (2011). Can GOCE help to improve temporal gravity field models? Presentation at: EGU General Assembly 2011, 04 -- 08 April 2011, Vienna, Austria

Contacts

Dipl.-Ing. Florian Heuberger, Institute of Theoretical Geodesy and Satellite Geodesy, TU Graz, Steyrergasse 30/III, 8010 Graz, Austria.

E-mail: florian.heuberger@tugraz.at

Dipl.-Ing. Daniel Rieser, Institute of Theoretical Geodesy and Satellite Geodesy, TU Graz, Steyrergasse 30/III, 8010 Graz, Austria.

E-mail: daniel.rieser@tugraz.at